PNAS RESEARCH ARTICLE | MICROBIOLOGY

The DedA superfamily member PetA is required for the transbilayer distribution of phosphatidylethanolamine in bacterial membranes

Ian J. Roney[a] and David Z. Rudner[a,1]

Edited by Natividad Ruiz, The Ohio State University, Columbus, Ohio; received February 3, 2023; accepted April 12, 2023 by Editorial Board Member Tina M. Henkin

The sorting of phospholipids between the inner and outer leaflets of the membrane bilayer is a fundamental problem in all organisms. Despite years of investigation, most of the enzymes that catalyze phospholipid reorientation in bacteria remain unknown. Studies from almost half a century ago in *Bacillus subtilis* and *Bacillus megaterium* revealed that newly synthesized phosphatidylethanolamine (PE) is rapidly translocated to the outer leaflet of the bilayer [Rothman & Kennedy, *Proc. Natl. Acad. Sci. U.S.A.* 74, 1821–1825 (1977)] but the identity of the putative PE flippase has eluded discovery. Recently, members of the DedA superfamily have been implicated in flipping the bacterial lipid carrier undecaprenyl phosphate and in scrambling eukaryotic phospholipids in vitro. Here, using the antimicrobial peptide duramycin that targets outward-facing PE, we show that *Bacillus subtilis* cells lacking the DedA paralog PetA (formerly YbfM) have increased resistance to duramycin. Sensitivity to duramycin is restored by expression of *B. subtilis* PetA or homologs from other bacteria. Analysis of duramycin-mediated killing upon induction of PE synthesis indicates that PetA is required for efficient PE transport. Finally, using fluorescently labeled duramycin we demonstrate that cells lacking PetA have reduced PE in their outer leaflet compared to wildtype. We conclude that PetA is the long-sought PE transporter. These data combined with bioinformatic analysis of other DedA paralogs argue that the primary role of DedA superfamily members is transporting distinct lipids across the membrane bilayer.

DedA | flippase | phosphatidylethanolamine | lipid transport | membrane biogenesis

Significance

How phospholipids get distributed between the inner and outer leaflets of biological membranes is poorly understood. While progress has been made in identifying transporters in eukaryotic cells, the identity of flippases in bacteria has remained elusive. Here, we provide evidence that the DedA superfamily member PetA is a lipid transporter that distributes phosphatidylethanolamine between the inner and outer leaflets of *Bacillus subtilis* membranes. Our work suggests that the primary role of DedA family members is in transporting distinct lipids across the membrane.

All bacterial cells are surrounded by an essential phospholipid membrane that contains its cytoplasmic contents, allows selective uptake of nutrients from the environment, enables respiration, and provides protection from external stresses. In addition to its barrier functions, phospholipids are also used as substrates in the synthesis and modification of surface polymers. In Gram-positive bacteria, phosphatidylglycerol (PG) headgroups are used in the synthesis of the anionic polymer lipoteichoic acid (1). In Gram-negative bacteria, PE is used as a substrate to modify lipid A (2). PG and PE are also required for the acylation of lipoproteins (3, 4). All of these reactions consume phospholipids from the outer leaflet of the cytoplasmic membrane. This leaflet also serves as a reservoir of phospholipids to populate the inner leaflet of the outer membrane in Gram-negative bacteria (5–7). Virtually all bacterial phospholipids are synthesized on the inner leaflet of the cytoplasmic membrane and are subsequently distributed across the lipid bilayer. How phospholipids are redistributed to sustain enzymatic activities and maintain membrane integrity remains poorly understood in all bacteria.

In a landmark paper published in 1977, James Rothman and Eugene Kennedy reported that the rate of transbilayer flipping of newly synthesized PE in *Bacillus subtilis* and *Bacillus megaterium* was greater than would be expected if PE flip-flop was spontaneous (8, 9). These findings led to the proposal that transbilayer movement was facilitated by membrane proteins (8, 10). Further support for this idea comes from studies in *Staphylococcus aureus* that revealed that MprF is a bifunctional synthase-flippase for lysyl-phosphatidylglycerol (LPG), a minor phospholipid species found in Gram-positive bacteria (11–13). MprF remains the only example of a bacterial phospholipid transporter.

Recent studies on the recycling of the lipid carrier undecaprenyl phosphate (UndP) that ferries most glycopolymers across the cytoplasmic membrane in bacteria, identified two families of UndP transporters (14, 15). One (UptA) is a member of the DedA superfamily, a broadly conserved but poorly understood family of membrane proteins found in all domains of life. Most bacterial genomes encode several DedA paralogs raising the possibility that these proteins could transport other lipids across the membrane. In support of this idea, in vitro studies on two eukaryotic DedA superfamily members, TMEM41B

Author affiliations: [a]Department of Microbiology, Harvard Medical School, Boston, MA 02115

Author contributions: I.J.R. designed research; I.J.R. performed research; I.J.R. and D.Z.R. analyzed data; and I.J.R. and D.Z.R. wrote the paper.

The authors declare no competing interest.

This article is a PNAS Direct Submission. N.R. is a guest editor invited by the Editorial Board.

[1]To whom correspondence may be addressed. Email: rudner@hms.harvard.edu.

This article contains supporting information online at https://www.pnas.org/lookup/suppl/doi:10.1073/pnas.2301979120/-/DCSupplemental.

Published May 8, 2023.

and VMP1, were found to redistribute phospholipids with diverse headgroups across the lipid bilayer in proteoliposomes (16, 17).

Here, we provide evidence that *B. subtilis* PetA, a DedA superfamily member, is the long-sought PE transporter proposed by Rothman and Kennedy almost a half century ago. We show that cells lacking PetA are more resistant to the antimicrobial peptide (AMP) duramycin that targets outward-facing PE and show that homologs from other bacteria can restore sensitivity to the Δ*petA* mutant. Using fluorescently labeled duramycin we demonstrate that cells lacking PetA have reduced PE in their outer leaflet compared to wildtype, but their total pools of PE are indistinguishable. Finally, we present bioinformatic analysis of bacterial proteins with domain fusions suggesting that DedA domains are capable of transporting diverse phospholipids. These findings combined with studies on the UndP transporter UptA and eukaryotic TMEM41B and VMP1 argue that the primary function of proteins in the DedA superfamily is transporting distinct lipids across the bilayer.

Results

ybfM Is in an Operon with Genes Involved in PE Biosynthesis. *B. subtilis* encodes six DedA paralogs. In recent work, we showed that one of them (UptA, formerly YngC) is an undecaprenyl phosphate (UndP) flippase that recycles the lipid carrier from the outer to the inner leaflet of the cytoplasmic membrane (14). We speculated that other members of this large protein family are transporters that act on distinct lipids. The *B. subtilis ybfM* gene encodes a DedA paralog and is co-expressed in an operon with *pssA* and *psd* that encode phosphatidylserine (PS) synthase and phosphatidylserine decarboxylase (Fig. 1*B*). These two enzymes are required for the synthesis of phosphatidylethanolamine (PE) (Fig. 1*A*). Genome neighborhood analysis revealed that *ybfM* is frequently present in an operon or adjacent to the PE biosynthetic genes (Fig. 1*B*). These findings led us to hypothesize that YbfM facilitates the transbilayer movement of PE. Based on the results described below, we have renamed *ybfM*, *petA* for PE transporter A.

PetA Expression Sensitizes Cells to Duramycin. To investigate whether PetA affects the distribution of PE between the inner and outer leaflets, we used the antimicrobial peptide duramycin. Duramycin is a 19 amino acid AMP that specifically binds PE and disrupts the membrane causing rapid cell death (18, 19). Importantly, duramycin and its derivatives have been shown to specifically bind surface-exposed PE and have been used to screen for phospholipid transporters (20) and detect PE asymmetries in yeast (21, 22). To test whether PetA affected surface-exposed PE, we used minimal inhibitory concentration (MIC) assays to compare the sensitivity of wildtype *B. subtilis* with strains lacking *petA* or the PE biosynthetic genes.

As reported previously, *pssA* and *psd* deletion strains were completely resistant to duramycin (19, 23) and the absence of LPG or cardiolipin did not affect the sensitivity of *B. subtilis* to duramycin (*SI Appendix*, Fig. S1), consistent with the specificity of duramycin for PE. Cells lacking PetA were twofold to fourfold more resistant to duramycin than wild-type (Fig. 2*A*), suggesting the mutant had less surface-exposed PE. Expression of *petA* in *trans* restored duramycin sensitivity to the Δ*petA* mutant, indicating that the deletion was not affecting expression of *pssA* or *psd*. Furthermore, expression of PetA homologs from diverse *Bacillus* species that displayed synteny with PE biosynthetic genes restored duramycin sensitivity to the *B. subtilis* Δ*petA* mutant (Fig. 2*C*). By contrast, overexpression of the DedA paralog UptA that transports UndP did not restore duramycin sensitivity to the Δ*petA* mutant (Fig. 2*C*).

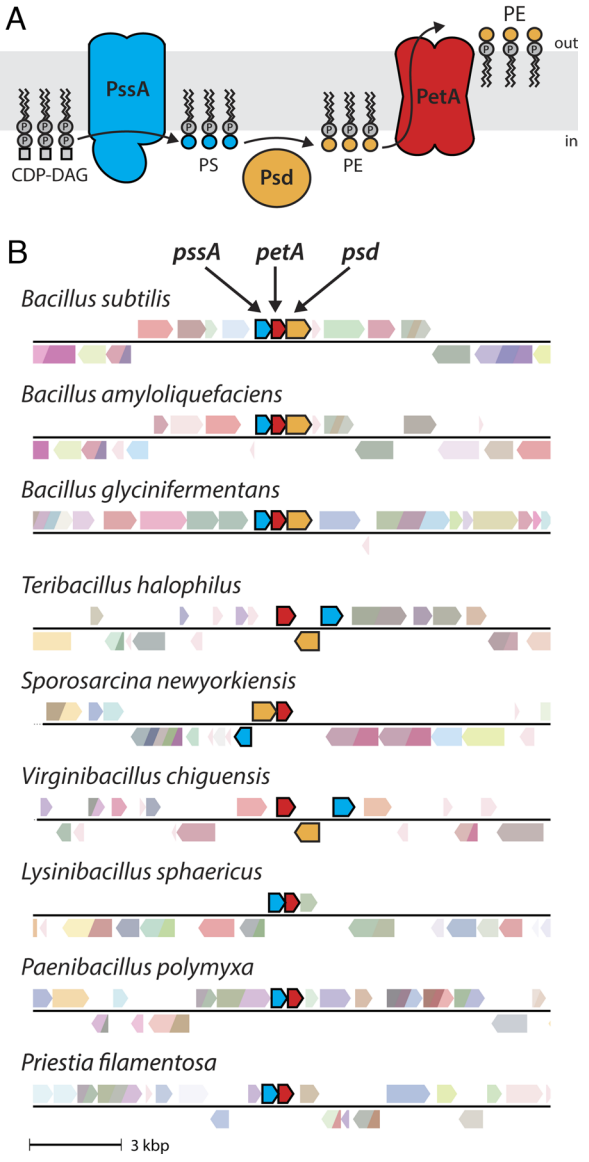

Fig. 1. *petA* genes are present adjacent to PE biosynthetic genes. (*A*) Schematic of the phosphatidylethanolamine (PE) biosynthetic pathway highlighting the role of PetA in transporting PE to the outer leaflet of the membrane. Phosphatidylserine synthase (PssA) catalyzes the synthesis of phosphotidylserine (PS) from CDP-diacylglycerol (CDP-DAG) and L-serine (not shown) in the inner leaflet of the cytoplasmic membrane. Phosphatidylserine decarboxylase (Psd) then converts PS into PE. PetA is proposed to flip PE to outer leaflet of the membrane. (*B*) Representative genomic neighborhood diagrams from *Bacillus* species showing the synteny of *petA*, *pssA*, and *psd*.

To rule out the possibility that the total PE pool is lower in the Δ*petA* mutant compared to wildtype, we analyzed the abundance of all major phospholipids using thin layer chromatography (TLC) (*SI Appendix*, Fig. S1). As previously reported (24), the Δ*pssA* and Δ*psd* mutants completely lacked PE, and the cells lacking Psd accumulated PS since PS could not be converted to PE (Figs. 1*A* and 2*B*). However, and importantly, the Δ*petA* mutant had PE levels that were comparable to wildtype and the *petA* complementation strain (Fig. 2*B* and *SI Appendix*, Fig. S1).

To further characterize the contribution of PetA to duramycin sensitivity, we deleted the entire *pssA-petA-psd* operon and reconstructed it at two neutral genomic loci. The *pssA* and *psd* genes were placed under the control of an IPTG (isopropyl-β-d-thiogalactopyranoside) -regulated promoter in strains with or without *petA* fused to a xylose-regulated

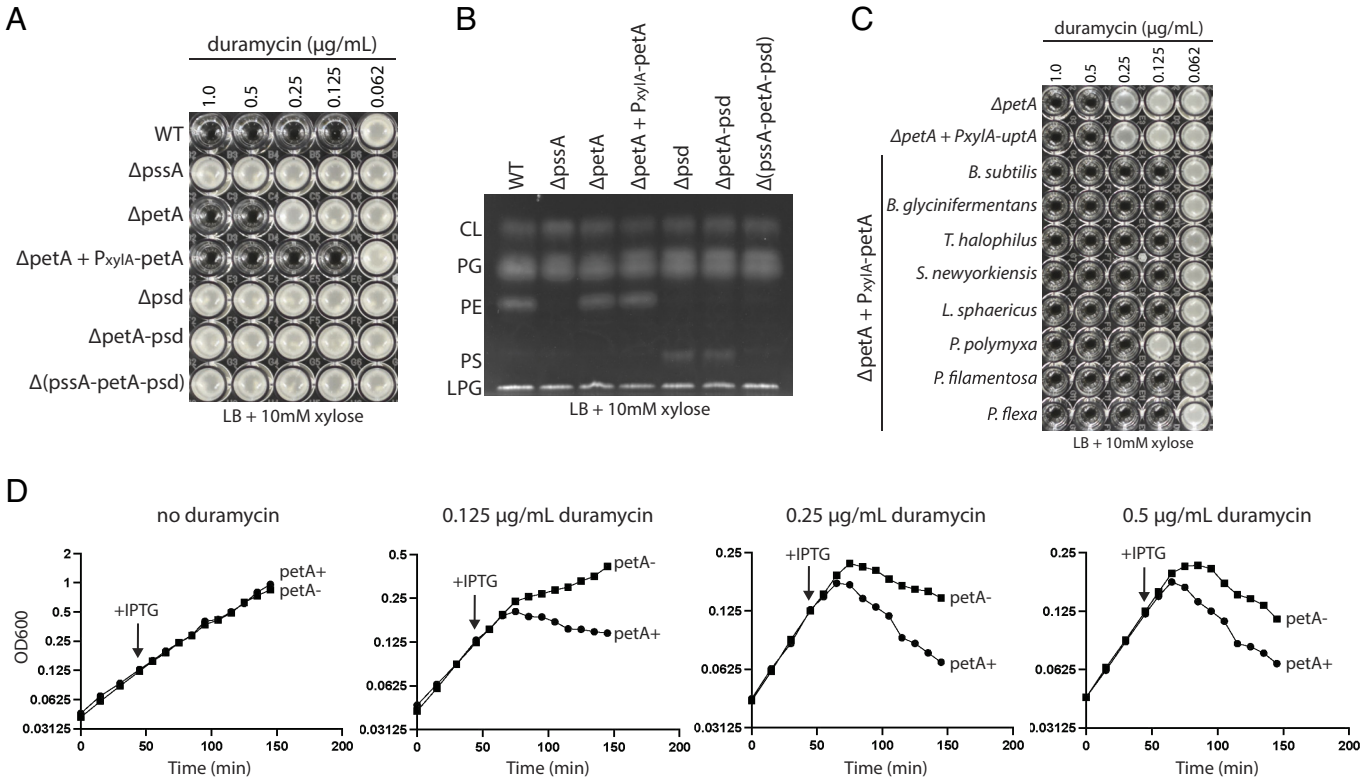

Fig. 2. *B. subtilis* cells lacking *petA* are more resistant to duramycin. (*A*) Representative duramycin MIC assay with the indicated *B. subtilis* strains. (*B*) TLC analysis of the strains in *A*. Cardiolipin (CL), phosphatidylglycerol (PG), phosphatidylethanolamine (PE), phosphatidylserine (PS), lysyl-phosphatidylglycerol (LPG) are shown. (*C*) MIC assay with *B. subtilis* Δ*petA* strains expressing PetA orthologs from the indicated bacterial species. (*D*) Growth curves in the presence of the indicated concentrations of duramycin of strains with *pssA* and *psd* expressed under IPTG control at a neutral genomic locus in the presence or absence of *petA* expressed under xylose control from a second neutral locus. The strains were grown in LB with 10 mM xylose and 20 μM IPTG was added at the indicated timepoint. IPTG, isopropyl-β-d-thiogalactopyranoside.

promoter (*SI Appendix*, Fig. S2*A*). These strains were grown with different concentrations of IPTG to titrate the levels of PE and analyzed for their sensitivity to duramycin. As expression of the PE synthesis enzymes increased, the sensitivity to duramycin of both the *petA*+ and *petA*– strains increased (*SI Appendix*, Fig. S2*B*) and at each IPTG concentration, the two strains had comparable levels of PE (*SI Appendix*, Fig. S2*C*). At every IPTG concentration tested the strain expressing PetA was more sensitive to duramycin (*SI Appendix*, Fig. S2*B*). The increased sensitivity ranged from 2- to 16-fold depending on the level of PE. As part of this analysis, we identified IPTG concentrations in which the strain lacking PetA produced more PE than the strain expressing PetA, yet the *petA*- strain was more resistant to duramycin (*SI Appendix*, Fig. S3). Since PE is synthesized on the inner leaflet of the membrane, these results argue that PetA functions in the transport of PE to outer leaflet of the membrane bilayer (Fig. 1*A*).

PetA Enhances the Rate of Appearance of Outward-Facing PE. In the seminal study of Rothman and Kennedy (8), newly synthesized PE in both *B. subtilis* and *B. megaterium* was rapidly flipped to the outer leaflet of the membrane at a rate greater than predicted if lipid flipflop were spontaneous. Motivated by these findings, we investigated whether the presence of PetA affects the rate that newly synthesized PE becomes exposed to the cell surface. Using the IPTG-regulated promoter fusion to *pssA* and *psd* described above, we induced de novo PE synthesis in cultures containing duramycin and monitored the rate at which the *petA*+ and *petA*- strains stopped growing and lysed (Fig. 2*D*). As anticipated, prior to IPTG addition and therefore in the absence of PE, the two strains grew identically and were completely resistant to duramycin (Fig. 2*D*). Upon addition of IPTG, both strains ceased growing and began to lyse. However, as can be seen in Fig. 2*D*, at all duramycin concentrations tested the *petA*+ strain was more rapidly killed than the *petA*- strain. We conclude that PetA increases the rate at which newly synthesized PE is distributed to the outer leaflet of the bilayer and is likely to be the long-sought transporter described by Rothman and Kennedy.

A Hydrophilic Pocket in the Predicted PetA Structure Is Critical for Function. To gain mechanistic insight into PetA transport activity, we turned to structural modeling. Alphafold predicts that PetA resembles a transporter with re-entrant helices on both sides of the phospholipid bilayer (Fig. 3*A*). These helices are predicted to generate a hydrophilic pocket within the membrane that could bind the zwitterionic PE headgroup, while allowing the hydrophobic lipid tails to remain in the bilayer during transport. Several of the residues that line the pocket are conserved among the PetA homologs that restored duramycin sensitivity to the *B. subtilis* Δ*petA* mutant (*SI Appendix*, Fig. S4*A*). To investigate whether these residues were important for function, we used a FLAG-tagged variant of the PetA homolog from *Teribacillus halophilus* (*Th*). The PetA(*Th*) protein was chosen because the epitope-tagged fusion was functional and readily detected by immunoblot (*SI Appendix*, Fig. S4 *B* and *C*). As can be seen in Fig. 3*B*, most of the conserved residues that line the hydrophilic pocket impaired the ability of the PetA(*Th*) to confer duramycin sensitivity. Importantly, all the mutant proteins were produced at levels similar to wildtype PetA(*Th*) (Fig. 3*C*). These data support

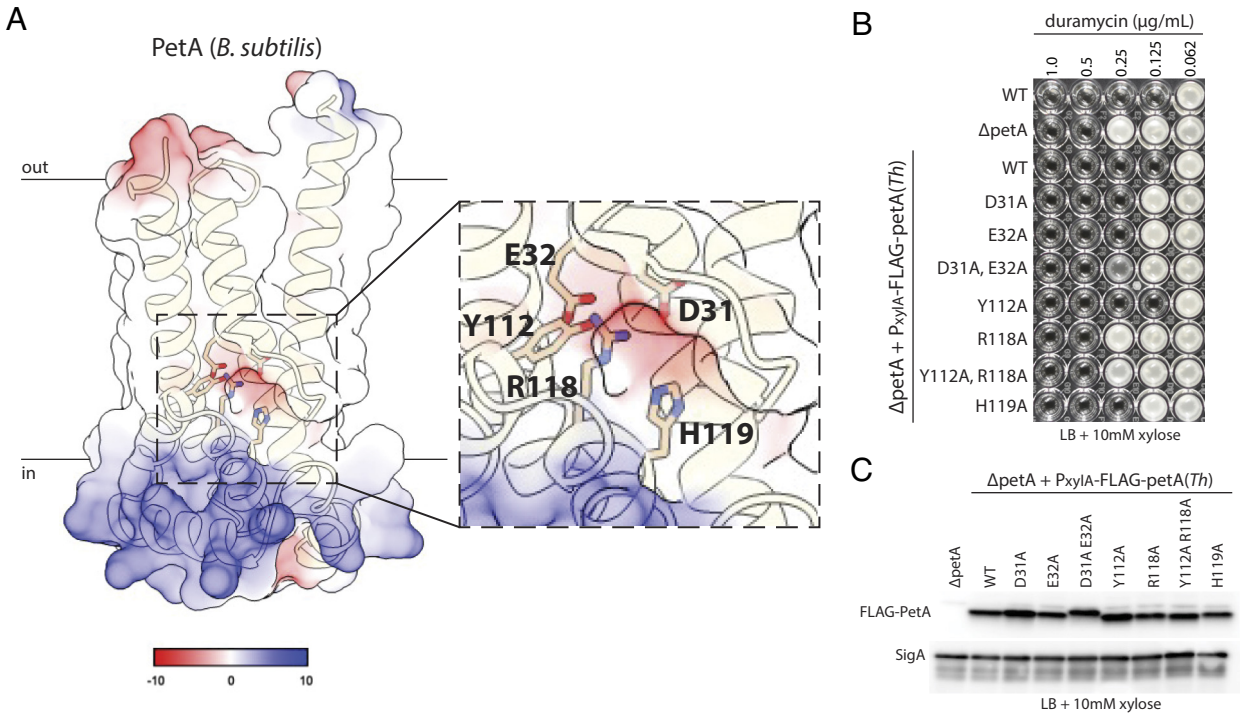

Fig. 3. A hydrophilic pocket in the predicted PetA structure is required for function. (*A*) Structural model of PetA predicted by AlphaFold2 colored based on surface charge distribution. Enlarged view of the hydrophilic pocket within the membrane is shown in the inset. Conserved residues, shown as sticks, are highlighted. (*B*) MIC assay of *B. subtilis* strains expressing the *T. halophilus* PetA ortholog with the indicated point mutants. (*C*) Representative immunoblot of the FLAG-PetA(*Th*) variants. SigA controls for loading.

the model that the hydrophilic pocket is important for PE transport and could bind the zwitterionic headgroup.

PetA Promotes Surface-Exposed PE. To more directly test whether PetA functions to increase surface-exposed PE, we turned to a fluorescent analog of duramycin (dura-FL) that has been used as a probe to quantify surface-exposed PE in both eukaryotic and bacterial cells (25, 26). First, we confirmed that dura-FL retains specificity for PE in *B. subtilis* membranes (*SI Appendix*, Fig. S5) and then and used it to probe PE localization. For the latter experiments, we used the strains described above in which the *pssA-petA-psd* operon was reconstructed at two neutral loci under inducible control. We grew strains with and without *petA* in the presence of 7.5 μM IPTG and 10 mM xylose. Under these conditions, cells lacking *petA* were 8-16-fold more resistant to duramycin than cells producing PetA (*SI Appendix*, Fig. S2*B*). Cells from exponentially growing cultures were stained with dura-FL and analyzed by fluorescence microscopy. The *petA*+ cells had markedly higher dura-FL labeling than the *petA*- cells (Fig. 4). Importantly, the membranes were intact under both conditions,

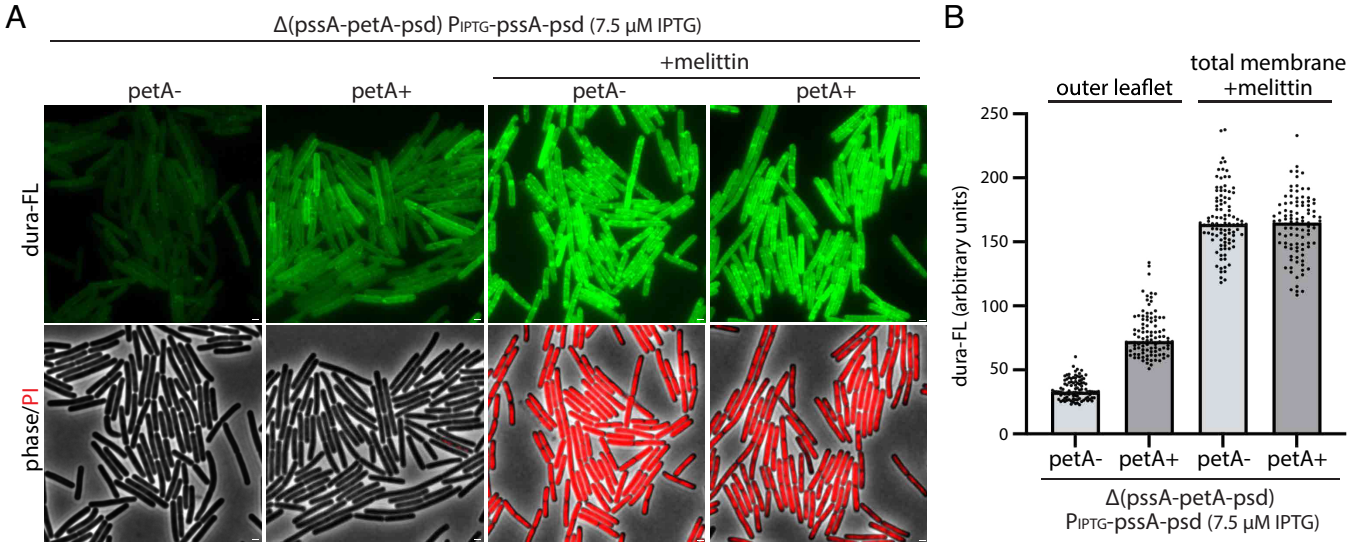

Fig. 4. PetA promotes surface exposure of PE. (*A*) Representative micrographs of the indicated *B. subtilis* strains stained with fluorescent duramycin (dura-FL) in the presence or absence of the membrane permeabilizing AMP, melittin. PssA and Psd were expressed with 7.5 μM IPTG in the presence of P_{xylA}-*petA* expressed with 10 mM xylose or in the absence of this inducible allele. *Top*, dura-FL staining. *Bottom*, overlays of phase-contrast and propidium iodide images. (Scale bar, 1 μm.) (*B*) Quantification of the dura-FL fluorescence from the strains shown in *A*. Bar represents median.

as assayed by propidium iodide, indicating that the dura-FL probe had not permeabilized the lipid bilayer and was therefore reporting on outward-oriented PE (Fig. 4*A*). To confirm that the cells grown in the presence and absence of PetA had equivalent amounts of PE, we performed the dura-FL labeling in the presence of melittin, a membrane permeabilizing AMP (27) that should allow dura-FL access to both the outer and inner leaflets of the membrane. As anticipated, virtually all cells stained with propidium iodide and had significantly higher dura-FL labeling. Importantly, the dura-FL labeling was similar in the presence and absence of PetA (Fig. 4).

Discussion

Altogether, our findings support the model that PetA catalyzes the transport of PE from the inner to the outer leaflet of the cytoplasmic membrane and likely represents the activity originally proposed by Rothman and Kennedy in 1977. The mechanism by which PetA flips PE is currently unknown, but our analysis of the residues predicted to line the hydrophilic pocket in PetA, suggests that this region binds the zwitterionic headgroup while the lipid tails remain in the bilayer. We speculate that PetA undergoes a conformational change upon PE binding that relocates this pocket toward the outer leaflet, reminiscent of the elevator-type mechanisms of small molecule transport across the bilayer (28). Future studies will be focused on investigating this and other models for PE flipping. It is noteworthy that PetA and UptA are predicted to have similar membrane topologies yet PetA functions in anterograde transport of PE and UptA in retrograde transport of UndP. The different directions of lipid transport of these related transporters suggest that DedA proteins are scramblases, serving as conduits that enable their lipid substrates to travel down their concentration gradients. Intriguingly, follow-up studies to Rothman and Kennedys' 1977 paper established that PE transport in both *Bacillus* cells and membrane extracts was energy independent (10, 29, 30). Furthermore, the eukaryotic DedA superfamily members, TMEM41B and VMP1, have been found to catalyze energy-independent scrambling of phospholipids in proteoliposomes (16, 17).

PetA represents the fourth DedA family member implicated in lipid transport and suggests that the primary role of the proteins in this superfamily is in lipid redistribution. Further support for this idea comes from bioinformatic analysis of bacterial proteins with domain fusions. This analysis identified several fusions of DedA domains to enzymatic domains involved in lipid synthesis and processing (Fig. 5). One set of fusions replaces the MprF flippase domain with a DedA domain, suggesting lysophosphosphotidylglycerol is synthesized and transported by these DedA-MprF fusions (Fig. 5*A*). Other examples include fusions of phospholipid synthase and phospholipase domains with DedA domains (Fig. 5 *B* and *C*). The challenge for the future is to identify the substrates flipped by these and other DedA family members. Recent attempts to classify DedA domain-containing proteins based on sequence conservation defined three main clades (31). YbfM/PetA was found to cluster with UptA homologs involved in UndP recycling rather than the clade predicted to be phospholipid flippases. Our data showing that PetA functions in PE transport, highlights the challenges that lie ahead in assigning functions to this diverse family of proteins.

We note that cells lacking *petA* were not fully resistant to duramycin, indicating that PetA transport is not the only mechanism that distributes PE to the outer leaflet of the membrane. We cannot rule out the possibility that there is a second dedicated PE transporter, but it is also possible that in the absence of PetA, PE is non-specifically redistributed by other lipid transporters or spontaneously flops, albeit slower than PetA-catalyzed redistribution. Furthermore, while our data establishes a role for PetA in PE transport, it is possible that PetA can transport other phospholipids. However, the number of DedA paralogs encoded by *B. subtilis* and other bacteria suggests a degree of specialization

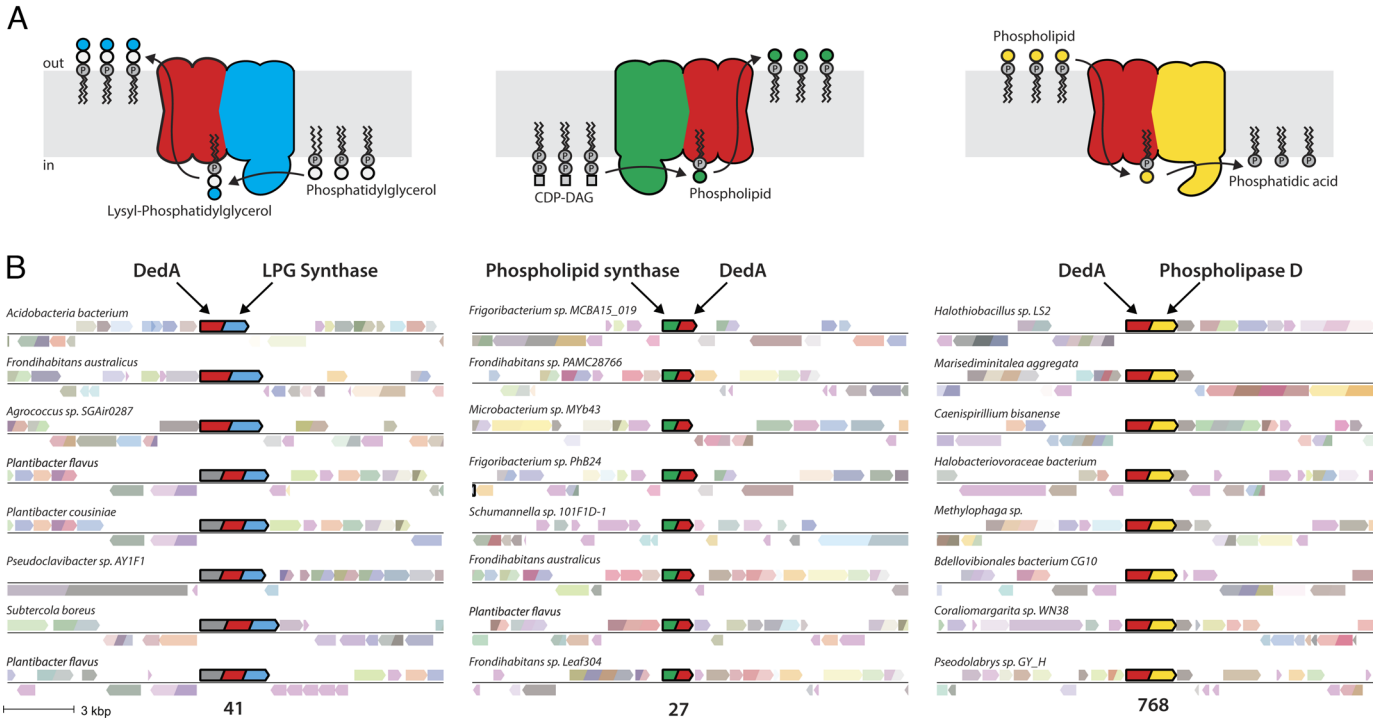

Fig. 5. Gene-fusion analysis suggests that DedA proteins are a widespread family of lipid flippases in bacteria. (*A*) Schematics of protein-fusions of DedA domains and domains with roles in lipid synthesis or modification. (*B*) Representative genomic neighborhood diagrams showing gene fusions of DedA with lysyl-phosphatidylglycerol (LPG) synthase, phospholipid synthase (CDP-OH phosphatidyltransferase) and phospholipase D domains. The number of gene fusions identified for each is indicated below the diagrams.

and a more narrow substrate specificity. We note that individual deletions of the other five *dedA* genes had no impact on duramycin sensitivity and a strain lacking all six paralogs had duramycin sensitivity that was indistinguishable from the single *petA* deletion (*SI Appendix*, Fig. S6). Thus, we suspect that PE transport is specific to PetA among the DedA family members in *B. subtilis*. Whether PE flipping is mediated by a member of another family of transporters or potentially occurs spontaneously remains an important area of investigation for the future.

Most of the phenotypic characterization of bacterial DedA proteins comes from work in *Escherichia coli*, which has 8 DedA paralogs. Individual mutants have mild or undetectable phenotypes but strains lacking two or more paralogs have pleiotropic phenotypes (32–35) that include impaired membrane potential (35) and changes in lipid composition (36). Gram-negative bacteria like *E. coli*, use phospholipids as substrates for the acylation of lipoproteins (3, 4), and the acylation and phosphoethanol modification of lipid A (2). These reactions occur in the outer leaflet of the cytoplasmic membrane. We hypothesize that defects in lipid sorting in the *E. coli* DedA mutants affect the rate of phospholipid consumption by these reactions and could explain the changes in membrane composition and defects in membrane potential observed.

Recent studies on the transport of phospholipids from the outer leaflet of the cytoplasmic membrane to the inner leaflet of the outer membrane in Gram-negative bacteria have revealed that AsmA family proteins act as bridges across the periplasmic space (*SI Appendix*, Fig. S7) (5–7). Interestingly, an AsmA-like protein in eukaryotes, Atg2, has been found to transport lipids from the endoplasmic reticulum (ER) to the developing autophagosome (*SI Appendix*, Fig. S7) (37). Furthermore, the DedA family members TMEM41b and VMP1 that scramble phospholipids in vitro directly interact with the Atg2 bridge at the ER membrane and are required for proper autophagosome formation (16, 17, 38–40). It is therefore tempting to speculate that in Gram-negative bacteria DedA family members function with AsmA bridge proteins to couple phospholipid flipping to the outer leaflet of the cytoplasmic membrane with transport across periplasmic space during OM biogenesis (*SI Appendix*, Fig. S7).

Methods

General Methods. All *B. subtilis* strains were derived from the prototrophic strain PY79 (41). All *B. subtilis* experiments were performed at 37 °C with aeration in lysogeny broth (LB). Antibiotic concentrations used were: 100 μg/mL spectinomycin, 10 μg/mL kanamycin, 5 μg/mL chloramphenicol, 10 μg/mL tetracycline, 1 μg/mL erythromycin and 25 μg/mL lincomycin (MLS). All *B. subtilis* strains were generated using the one-step competence method unless indicated otherwise. All strains, plasmids, oligonucleotides, and synthetic DNA used in this study can be found in *SI Appendix*, Tables S3–S6.

MIC Assays. Exponentially growing cultures of *B. subtilis* were back-diluted 1:10,000 into 96-well microtiter plates containing the indicated concentrations of antibiotic and inducers. Plates were sealed with breathable membranes and grown with orbital shaking at 37 °C overnight. Plates were photographed after the overnight (~16 h) incubation. All MIC assays were performed in at least triplicate and representative images are shown. All replicates gave comparable results. Full details on all replicate experiments can be found in *SI Appendix*, Table S2.

Growth Curve Assays. Exponentially growing cultures of *B. subtilis* were back-diluted to a starting OD of 0.05 in 25 mL LB containing 10 mM xylose and the indicated concentration of duramycin in 250-mL baffled flasks. Cultures were grown for 45 min with shaking with samples taken for OD measurements every 15 min. After 45 min of growth, IPTG was added to a final concentration of 20 μM and OD measurements were taken every 10 min thereafter. Growth curves were plotted with GraphPad Prism. Growth curves were performed at least three times and representative graphs are shown. All replicates gave comparable results.

Genomic Neighborhood and Domain Fusion Analysis. Gene neighborhood analysis was performed as previously described (14). Briefly, the Enzyme Similarity Tool (42) (EFI-EST v2.0) from the Enzyme Function Initiative (available at: https://efi.igb.illinois.edu/efi-est/) was used to generate sequence similarity networks (SSN) for the DedA protein family from the pfam entry SNARE_assoc (PF09335). Due to the large size of the SNARE_assoc family, the UniRef90 database was used. The SSN was then used as input for performing genomic neighborhood analysis using the Enzyme Function Initiative Genome Neighborhood Tool (EFI-GNT v1.0) available at: https://efi.igb.illinois.edu//efi-gnt/index.php. Alignment score cutoff of 35% was used for the analysis. Gene neighborhood diagrams were generated to visualize the 10 nearest genes surrounding all *dedA* genes. Domain fusions were identified for the PF09335(SNARE_assoc) protein family on the InterPro website available at: https://www.ebi.ac.uk/interpro/entry/pfam/PF09335/.

Duramycin-FL Labeling and Fluorescence Microscopy. Exponentially growing cultures of *B. subtilis* were collected by centrifugation at 7000 RPM for 2 min. Cells were washed once with 1× PBS (pH 7.4) and resuspended in 1/25th volume of 1× PBS. Duramycin-LC-Fluorescein (Dura-FL) (Molecular Targeting Technologies) was added to a final concentration of 25 μM and incubated for 30 s. Cells were washed with 1× Phosphate Buffered Saline (PBS), resuspended in 1/25th volume of 1× PBS, and spotted onto 1.5% agarose pads containing growth medium. Propidium iodide labeling was performed in 1xPBS at final concentrations of 5 μM. To permeabilize membranes, melittin was added to a final concentration of 20 μg/mL during the dura-FL labeling step.

Phase-contrast and fluorescence microscopy was performed with a Nikon Ti inverted microscope using a Plan Apo 100×/1.4 Oil Ph3 DM objective, a Lumencore SpectraX Light Emitting Diode illumination system and an Andor Zyla 4.2 Plus sCMOS camera. Chroma ET filter cubes (#49002 and 49008) were used for imaging, dura-FL and propidium iodide, respectively. Exposure time of 1 s was used for dura-FL and 50 ms was used for propidium iodide. Images were acquired with Nikon elements 4.3 software and analyzed using ImageJ (version2.3). Images were taken from multiple fields of view and images shown are representative of at least three independent experiments.

Fluorescence Microscopy Quantification. ImageJ was used to quantify fluorescent intensities of dura-FL labeling. Cell boundaries were identified by thresholding the dura-FL images to distinguish cells from background. Intensity values from single cells in the dura-FL channel were extracted and the background autofluorescence from an empty field of view was subtracted from the image. Data from 100 cells was plotted using GraphPad Prism 9.

Structural Model Visualization. Alphafold2 predictions of PetA were downloaded from the AlphaFold Protein Structure Database (available at: https://alphafold.ebi.ac.uk/). ChimeraX1.3 was used to visualize the structural models and generate images. Residues critical for PetA function are shown as sticks.

Immunoblot Analysis. Immunoblot analysis was performed as described previously (43). Briefly, 1 mL of exponentially growing cells were normalized by OD600 and harvested by centrifugation (2 min at 7,000 RPM). The cell pellet was resuspended in lysis buffer (20 mM Tris pH 7.0, 10 mM $MgCl_2$, 1mM EDTA, 1 mg/mL lysozyme, 10 μg/mL DNase I, 100 μg/mL RNase A, 1 mM PMSF, 1 μg/mL leupeptin, 1 μg/mL pepstatin) and incubated at 37 °C for 15 min. An equal volume of sample buffer (0.25 M Tris pH 6.8, 4% SDS, 20% glycerol, 10 mM EDTA, 10% β-mercaptoethanol) was added to the lysis reactions and vortexed briefly to complete lysis. Proteins were separated by SDS- PAGE on 15% polyacrylamide gels, transferred onto Immobilon-P membranes (Millipore) by electrophoretic transfer and blocked with 5% Milk in phosphate buffered saline with 0.5% Tween-20 (PBS-T). The blocked membranes were probed with polyclonal anti-FLAG (1:3,000) (Sigma Aldrich) or polyclonal anti-SigA (1:10,000) antibodies diluted into 3% BSA in PBS-T. Primary antibodies were detected using horseradish peroxidase-conjugated goat antirabbit IgG (1:3,000) (BioRad) or goat antimouse IgG (1:20,000) (BioRad) and the Super Signal chemiluminescence reagent as described by the manufacturer (Pierce). Immunoblot analyses shown are representative of two biological replicates. All replicates gave comparable results.

Multiple Sequence Alignment. Multiple sequence alignments were performed using Clustal Omega version 1.2.4 (44) and visualized with Espript 3.0 (45).

Lipid Extractions. Three OD units of exponentially growing cultures of *B. subtilis* were collected by centrifugation at 3200xg for 5 min. Cells were washed once with 1 mL of 1× PBS (pH 7.4) and resuspended in 1xPBS (pH 7.4) to a final volume of 300 μL. 750 μL of methanol and 375 μL of chloroform were added to cells (1:2:0.8) (CHCl3:MeOH:H2O). The mixture was incubated at room temperature for 1 h with occasional vortexing. The mixture was then centrifuged at 2000xg for 10 min at 4° C to remove debris. The supernatant was added to a clean test tube with 375 μL chloroform and 375 μL of water (1:1:0.9) (CHCl3:MeOH:H2O) and incubated at room temperature for 10 min with occasional vortexing. Finally, the mixture was centrifuging at 2000× *g* for 10 min at 4° C. The organic phase was removed and dried under vacuum.

Thin-Layer Chromatography. The chromatography chamber was lined with Whatman paper and equilibrated for 2 h with chloroform–methanol–acetic acid (65:25:8, v/v). Silica 60 TLC plates (Supelco) were impregnated for 1 min in a 1.2% boric acid solution in 100% ethanol and activated at 100° C for 30 min. Dried lipid samples were resuspended in 5 μL of chloroform and 3 μL was immediately spotted onto the activated TLC plate and allowed to dry. The TLC plate was placed in the chromatography chamber until the solvent front was approximately 1 inch from top of the plate. The TLC plate was air dried and briefly submerged in primuline (5 mg/100 mL in 80:20 acetone–water) and then imaged under ultraviolet light. Images shown are representative of three biological replicates. All replicates gave comparable results.

Data, Materials, and Software Availability. Uncropped immunoblots are included in the supplementary information. Uniprot accession codes for gene neighborhood analysis can be found in supplementary tables. Primers, synthetic DNA constructs and strains used can be found in supplementary tables. All study data are included in the article and/or *SI Appendix*.

ACKNOWLEDGMENTS. We thank all members of the Bernhardt-Rudner supergroup for helpful advice, discussions, and encouragement and the MicRoN core for advice on microscopy. Support for this work comes from the NIH Grants R35GM145299 and U19 AI158028 (D.Z.R.).

1. A. Gründling, O. Schneewind, Synthesis of glycerol phosphate lipoteichoic acid in staphylococcus aureus. *Proc. Natl. Acad. Sci. U.S.A.* **104**, 8478–8483 (2007).
2. M. S. Trent, Biosynthesis, transport, and modification of lipid A. *Biochem. Cell Biol.* **82**, 71–86 (2004).
3. S. Jackowski, C. O. Rock, Transfer of fatty acids from the 1-position of phosphatidylethanolamine to the major outer membrane lipoprotein of escherichia coli. *J. Biol. Chem.* **261**, 11328–11333 (1986).
4. K. Sankaran, H. C. Wu, Lipid modification of bacterial prolipoprotein. Transfer of diacylglyceryl moiety from phosphatidylglycerol. *J. Biol. Chem.* **269**, 19701–19706 (1994).
5. N. Ruiz, R. M. Davis, S. Kumar, YhdP, TamB, and YdbH Are redundant but essential for growth and lipid homeostasis of the gram-negative outer membrane. *Mbio* **12**, e0271421 (2021).
6. M. V. Douglass, A. B. McLean, M. S. Trent, Absence of YhdP, TamB, and YdbH leads to defects in glycerophospholipid transport and cell morphology in Gram-negative bacteria. *Plos Genet.* **18**, e1010096 (2022).
7. J. Grimm *et al.*, The inner membrane protein YhdP modulates the rate of anterograde phospholipid flow in escherichia coli. *Proc. Natl. Acad. Sci. U.S.A.* **117**, 26907–26914 (2020).
8. J. E. Rothman, E. P. Kennedy, Rapid transmembrane movement of newly synthesized phospholipids during membrane assembly. *Proc. Natl. Acad. Sci. U.S.A.* **74**, 1821–1825 (1977).
9. H. M. McConnell, R. D. Kornberg, Inside-outside transitions of phospholipids in vesicle membranes. *Biochemistry* **10**, 1111–1120 (1971).
10. S. Hrafnsdóttir, J. W. Nichols, A. K. Menon, Transbilayer movement of fluorescent phospholipids in bacillus megaterium membrane vesicles †. *Biochemistry* **36**, 4969–4978 (1997).
11. C. M. Ernst *et al.*, The bacterial defensin resistance protein MprF consists of separable domains for lipid lysinylation and antimicrobial peptide repulsion. *Plos Pathog.* **5**, e1000660 (2009).
12. C. M. Ernst *et al.*, The lipid-modifying multiple peptide resistance factor is an oligomer consisting of distinct interacting synthase and flippase subunits. *Mbio* **6**, e0234014 (2015).
13. D. Song, H. Jiao, Z. Liu, Phospholipid translocation captured in a bifunctional membrane protein MprF. *Nat. Commun.* **12**, 2927 (2021).
14. I. J. Roney, D. Z. Rudner, Two broadly conserved families of polyprenyl-phosphate transporters. *Nature* **613**, 729–734 (2023).
15. B. Sit *et al.*, Undecaprenyl phosphate translocases confer conditional microbial fitness. *Nature* **613**, 721–728 (2023).
16. Y. E. Li *et al.*, TMEM41B and VMP1 are scramblases and regulate the distribution of cholesterol and phosphatidylserine. *J. Cell Biol.* **220**, e202103105 (2021).
17. D. Huang *et al.*, TMEM41B acts as an ER scramblase required for lipoprotein biogenesis and lipid homeostasis. *Cell Metab.* **33**, 1655–1670.e8 (2021).
18. K. Iwamoto *et al.*, Curvature-dependent recognition of ethanolamine phospholipids by duramycin and cinnamycin. *Biophys. J.* **93**, 1608–1619 (2007).
19. J. Navarro *et al.*, Interaction of duramycin with artificial and natural membranes. *Biochemistry* **24**, 4645–4650 (1985).
20. U. Kato *et al.*, A novel membrane protein, Ros3p, is required for phospholipid translocation across the plasma membrane insaccharomyces cerevisiae *. *J. Biol. Chem.* **277**, 37855–37862 (2002).
21. E. Quon *et al.*, Endoplasmic reticulum-plasma membrane contact sites integrate sterol and phospholipid regulation. *Plos Biol.* **16**, e2003864 (2018).
22. K. Nakano, T. Yamamoto, T. Kishimoto, T. Noji, K. Tanaka, Protein kinases Fpk1p and Fpk2p are novel regulators of phospholipid asymmetry. *Mol. Biol. Cell* **19**, 1783–1797 (2008).
23. C. Bordi *et al.*, In vitro mutagenesis of bacillus subtilis by using a modified Tn 7 transposon with an outward-facing inducible promoter. *Appl. Environ. Microb.* **74**, 3419–3425 (2008).
24. L. I. Salzberg, J. D. Helmann, Phenotypic and transcriptomic characterization of bacillus subtilis mutants with grossly altered membrane composition. *J. Bacteriol.* **190**, 7797–7807 (2008).
25. M. Zhao, Lantibiotics as probes for phosphatidylethanolamine. *Amino. Acids* **41**, 1071–1079 (2011).
26. S. Hasim *et al.*, Elucidating duramycin's bacterial selectivity and mode of action on the bacterial cell envelope. *Front. Microbiol.* **9**, 219 (2018).
27. M.-T. Lee, T.-L. Sun, W.-C. Hung, H. W. Huang, Process of inducing pores in membranes by melittin. *Proc. Natl. Acad. Sci. U.S.A.* **110**, 14243–14248 (2013).
28. A. A. Garaeva, D. J. Slotboom, Elevator-type mechanisms of membrane transport. *Biochem. Soc. T.* **48**, 1227–1241 (2020).
29. K. E. Langley, E. P. Kennedy, Energetics of rapid transmembrane movement and of compositional asymmetry of phosphatidylethanolamine in membranes of bacillus megaterium. *Proc. Natl. Acad. Sci. U.S.A.* **76**, 6245–6249 (1979).
30. S. Hrafnsdóttir, A. K. Menon, Reconstitution and partial characterization of phospholipid flippase activity from detergent extracts of the bacillus subtilis cell membrane. *J. Bacteriol.* **182**, 4198–4206 (2000).
31. H. Todor, N. Herrera, C. Gross, Three bacterial DedA subfamilies with distinct functions and phylogenetic distribution. *mBio* **14**, e0002823 (2023).
32. L. A. Boughner, W. T. Doerrler, Multiple deletions reveal the essentiality of the DedA membrane protein family in escherichia coli. *Microbiology* **158**, 1162–1171 (2012).
33. R. Sikdar, W. T. Doerrler, Inefficient tat-dependent export of periplasmic amidases in an escherichia coli strain with mutations in two deda family genes. *J. Bacteriol.* **192**, 807–818 (2010).
34. S. Kumar, W. T. Doerrler, Escherichia coli YqjA, a member of the conserved DedA/Tvp38 membrane protein family, is a putative osmosensing transporter required for growth at alkaline pH. *J. Bacteriol.* **197**, 2292–2300 (2015).
35. S. Kumar, W. T. Doerrler, Members of the conserved DedA family are likely membrane transporters and are required for drug resistance in escherichia coli. *Antimicrob. Agents Chemother.* **58**, 923–930 (2014).
36. K. Thompkins, B. Chattopadhyay, Y. Xiao, M. C. Henk, W. T. Doerrler, Temperature sensitivity and cell division defects in an escherichia coli strain with mutations in yghB and yqjA, encoding related and conserved inner membrane proteins. *J. Bacteriol.* **190**, 4489–4500 (2008).
37. D. P. Valverde *et al.*, ATG2 transports lipids to promote autophagosome biogenesis. *J. Cell Biol.* **218**, 1787–1798 (2019).
38. A. Ghanbarpour, D. P. Valverde, T. J. Melia, K. M. Reinisch, A model for a partnership of lipid transfer proteins and scramblases in membrane expansion and organelle biogenesis. *Proc. Natl. Acad. Sci. U.S.A.* **118**, e2101562118 (2021).
39. F. Moretti *et al.*, TMEM41B is a novel regulator of autophagy and lipid mobilization. *Embo. Rep.* **19**, e45889 (2018).
40. C. J. Shoemaker *et al.*, CRISPR screening using an expanded toolkit of autophagy reporters identifies TMEM41B as a novel autophagy factor. *Plos Biol.* **17**, e2007044 (2019).
41. P. Youngman, J. B. Perkins, R. Losick, Construction of a cloning site near one end of Tn917 into which foreign DNA may be inserted without affecting transposition in bacillus subtilis or expression of the transposon-borne erm gene. *Plasmid* **12**, 1–9 (1984).
42. R. Zallot, N. Oberg, J. A. Gerlt, The EFI web resource for genomic enzymology tools: Leveraging protein, genome, and metagenome databases to discover novel enzymes and metabolic pathways. *Biochemistry* **58**, 4169–4182 (2019).
43. X. Wang *et al.*, Condensin promotes the juxtaposition of DNA flanking its loading site in bacillus subtilis. *Gene. Dev.* **29**, 1661–1675 (2015).
44. F. Sievers *et al.*, Fast, scalable generation of high-quality protein multiple sequence alignments using clustal omega. *Mol. Syst. Biol.* **7**, 539–539 (2011).
45. X. Robert, P. Gouet, Deciphering key features in protein structures with the new ENDscript server. *Nucleic Acids Res.* **42**, W320–W324 (2014).